

ChemComm

Accepted Manuscript

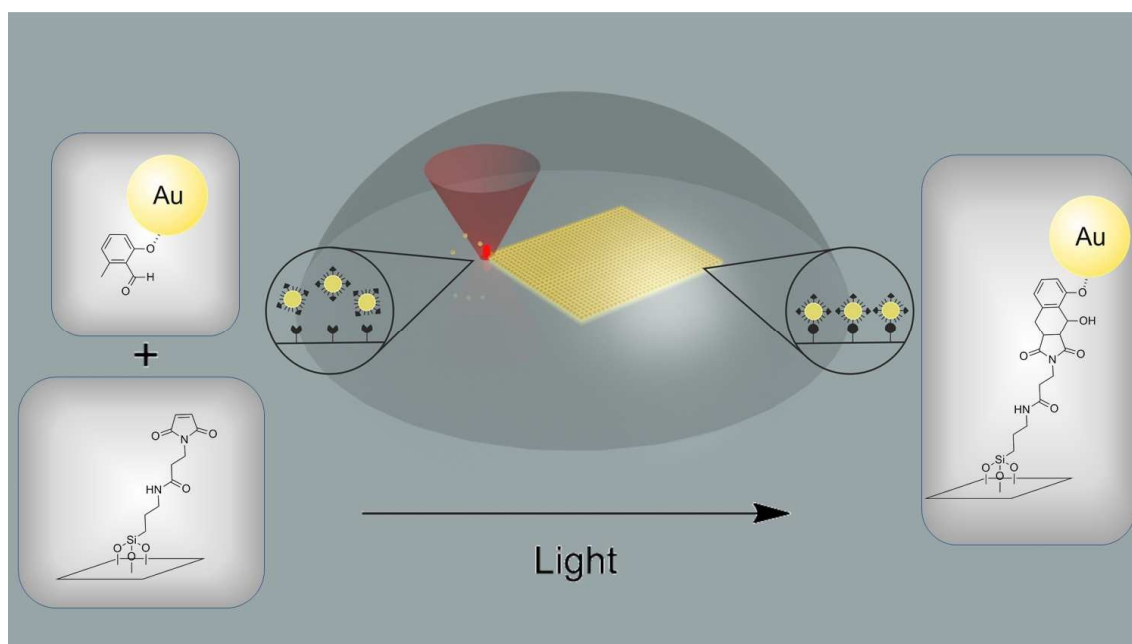


This is an *Accepted Manuscript*, which has been through the Royal Society of Chemistry peer review process and has been accepted for publication.

Accepted Manuscripts are published online shortly after acceptance, before technical editing, formatting and proof reading. Using this free service, authors can make their results available to the community, in citable form, before we publish the edited article. We will replace this *Accepted Manuscript* with the edited and formatted *Advance Article* as soon as it is available.

You can find more information about *Accepted Manuscripts* in the [Information for Authors](#).

Please note that technical editing may introduce minor changes to the text and/or graphics, which may alter content. The journal's standard [Terms & Conditions](#) and the [Ethical guidelines](#) still apply. In no event shall the Royal Society of Chemistry be held responsible for any errors or omissions in this *Accepted Manuscript* or any consequences arising from the use of any information it contains.



Writing with Gold: A photolithographic approach for the spatially resolved surface encoding of photoreactive gold nanoparticles is shown to enable the generation of highly defined gold surface patterns.

Cite this: DOI: 10.1039/c0xx00000x

www.rsc.org/xxxxxx

ARTICLE TYPE

Photo-Induced Surface Encoding of Gold Nanoparticles

Lukas Stolzer,^{a,b} Alexander S. Quick,^{b,c} Doris Abt,^{b,c} Alexander Welle,^{b,c} Denys Naumenko,^{d,e} Marco Lazzarino,^d Martin Wegener,^f Christopher Barner-Kowollik^{*b,c} and Ljiljana Fruk^{*a}

Received (in XXX, XXX) Xth XXXXXXXXX 20XX, Accepted Xth XXXXXXXXX 20XX

DOI: 10.1039/b000000x

Photoreactive gold nanoparticles (NP) can be encoded in a spatially resolved fashion using direct laser writing techniques into variable patterns. The surface of the gold nanoparticles is imparted with photoreactivity by tethering photo-caged dienes ('photoenols'), which are able to undergo a rapid Diels-Alder cycloaddition with surface anchored enes. Subsequent to surface encoding, the particles feature residual caged dienes, which can be reactivated for secondary surface encoding.

In the past decade, the modification and application of engineered nanomaterials, in particular variable types of functional metallic nanoparticles (NP), have attracted growing interest. Besides their numerous biomedical applications, i.e. for the design of biosensing or diagnostic/therapeutic platforms,¹⁻³ initial expectations for their use for the preparation of novel plasmonic and optoelectronic devices have not yet been fulfilled. This is mainly due to the obstacles posed by NP assembly and patterning, such as the preparation of micron- and submicron assemblies essential for electronic, optical and sensor applications.⁴⁻⁶ Both top-down approaches such as lithography as well as bottom-up approaches based on various chemical strategies have been employed to prepare variable patterns of NPs. In recent years, a number of studies focused on the combination of both methodologies often using van der Waals and electrostatic interactions or covalent bonding jointly with lithography based techniques to fabricate functional structures in well-defined patterns. For instance, Rotello and co-workers prepared photoactivatable Au NPs containing UV cleavable protecting groups and fabricated patterns *via* photolithography and electrostatic assembly based on surface charging after a protecting group cleavage.⁷ A different approach based on chemical electron beam lithography was reported by Mendes *et al.* Using silica wafers with immobilized nitro groups, electrostatic binding of citrate-capped Au NPs was achieved after the reduction of nitro to amine groups and additional protonation.⁸ However, despite the initial success of the electrostatically driven assembly, the chemically directed assembly using covalent ligation strategies – which results in stronger and specific binding – is preferred for electronic applications involving high electric fields.⁹ Such a covalent approach based on Huisgen 1,3-dipolar cycloadditions and microcontact printing (μ CP) was previously used to design patterns of dyes,¹⁰ and also biomolecules such as proteins¹¹ and

DNA.¹² Recently, the strategy was expanded to immobilize azide functionalized Au NPs onto alkyne coated Au surfaces.¹³ However, μ CP has limitations as it is based on the use of pre-patterned stamps and their deformation as well as the spreading of ink lead to blurring of the desired pattern.¹⁴ In addition, μ CP is only applicable to flat surfaces and generally does not allow for temporal control. To address the general lack of covalent surface encoding strategies for NPs and the disadvantages associated with μ CP, we herein report the rapid encoding of NPs employing a light-induced cycloaddition based on photo-caged dienes and direct laser writing (DLW) to achieve both spatial and temporal control over NP pattern design (Fig. 1). DLW is a powerful tool for the fabrication of complex structures and it can employ both continuous-wave and a pulsed laser.¹⁵ By moving the laser beam either through a photoresist or – alternatively – over a surface, multiphoton absorption can lead to a photoreaction at specific positions.¹⁶ This principle in combination with light induced ligation strategies has already been employed to fabricate 3D microstructures.¹⁷

Recently, we have shown that the light-induced Diels-Alder cycloaddition of photocaged dienes (*o*-quinodimethanes or photoenols) and maleimides, which fulfill the strict requirements

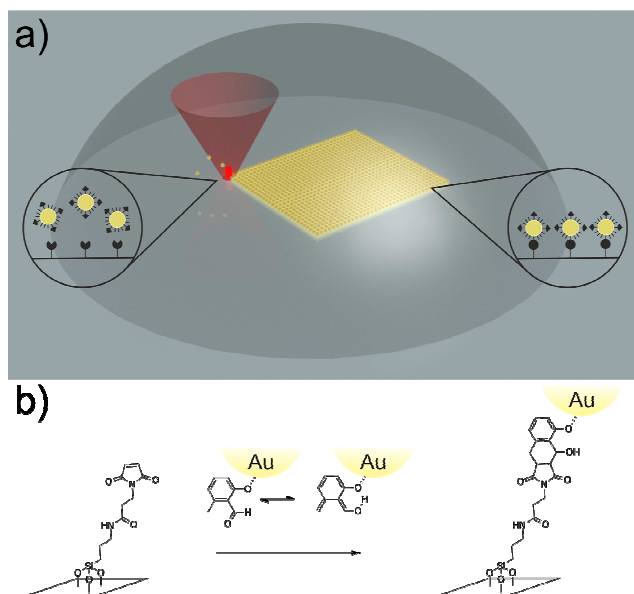


Fig. 1 a) Scheme of the photo-induced surface assembly of Au NPs employing DLW. (b) Light triggered Diels Alder reaction of the photo-generated *o*-quinodimethane located on the Au NPs with surface anchored maleimides.

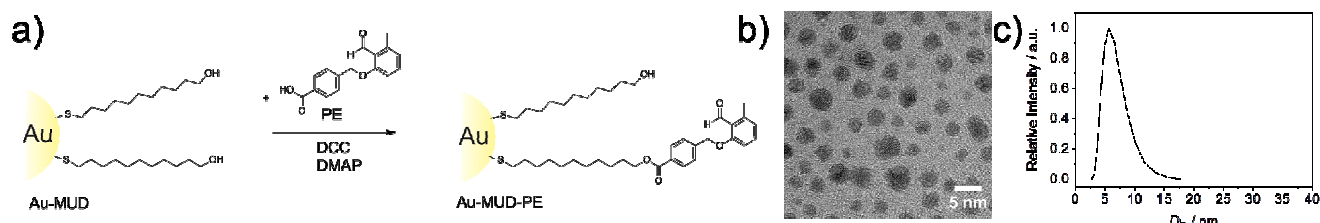


Fig. 2 (a) Preparation of photoenol (PE) containing Au NPs (**Au-MUD-PE**) *via* esterification. (b) HRTEM image of **Au-MUD-PE**. (c) Volume average size distribution obtained *via* DLS of **Au-MUD-PE**.

of click chemistry,¹⁸ can be employed for the functionalization of various surfaces, including silver NPs.¹⁹⁻²¹ Upon irradiation, the *o*-quinodimethane precursor molecules undergo intramolecular hydrogen abstraction followed by bond reorganization to form highly reactive dienes which allow Diels-Alder reaction with electron deficient alkenes.²²

Within the current study, we present the combination of both top-down and bottom-up approaches, first preparing photoenol modified Au NPs and subsequently using DLW to afford 2D spatially resolved encoding of the photoactivatable Au NPs (Fig. 1), which can additionally be modified after patterning. The direct one-pot synthesis of photoenol functional Au NPs using an Au salt precursor and a variety of different reducing agents was not possible as the photoenol moiety is not compatible with reducing agents due to the reduction of aldehydes to hydroxyl functions, resulting in the loss of reactivity.²¹ To circumvent this issue, first, stable mercaptoundecanol (MUD)-capped Au NPs (**Au-MUD**) were synthesized according to a literature procedure²³ and the photoenol moiety was subsequently introduced *via* the esterification of the MUD ligands (Fig. 2a). The obtained photoenol modified **Au-MUD-PE** were characterized by high-resolution transmission electron microscopy (HRTEM) (Fig. 2b), dynamic light scattering (DLS, Fig. 2c), FT-IR and ¹H-NMR spectroscopy, indicating that NPs with 3.02 ± 0.74 nm (Fig. S17) in size were coated with –on average – 209 MUD ligands (Fig. S3). The amount of photoenol on the particle surface *via* ¹H-NMR was close to 5% of the total number of ligands (equivalent to approx. 10 photoenol groups per particle, Fig. S3).

In order to obtain precisely encoded patterns *via* DLW, a covalent strategy compatible with both multiphoton process and Au NPs (to avoid aggregation or destruction of crystalline core) was employed. We first assessed the potential of the photoenol based Diels-Alder reaction by employing the MUD-PE linker for a test reaction with maleimide. A reaction mixture was irradiated in dimethylformamide (DMF) and subsequent analysis by ESI-MS evidenced a new peak series, which was assigned to the product of the light-induced Diels-Alder reaction, indicating the complete conversion to the photoadduct without any side-product formation (ESI, Fig. S7).

After confirming that the light induced Diels-Alder cycloaddition is a fast and efficient covalent strategy for Au NP modification, patterns of Au NPs on glass surfaces were designed *via* direct DLW encoding. First, a glass surface was modified with maleimide groups in a two step approach employing (3-aminopropyl)triethoxysilane (APTES) and 4-maleimidobutryl chloride as previously reported.²⁴ Subsequently, photoenol Au NPs were patterned in square patterns ($20 \mu\text{m} \times 20 \mu\text{m}$) (refer to Fig. 1) using DLW.

It should be noted that UV-A light (315-400 nm) for the test reaction of MUD-PE linker and maleimide was used to phototrigger the reaction ($\lambda_{\text{max}} = 320$ nm). Control studies indicated that Au NPs are stable under these conditions for several hours (no agglomeration was observed by UV-Vis spectroscopy, Fig. S10). Nevertheless, it has been shown that laser irradiation of thiol-passivated Au NPs with UV-A wavelengths may lead to agglomerated Au NPs.²⁵ Thus, we employed a multiphoton process to activate the photoenol moiety with a 700 nm pulsed laser. To ensure that there is no undesired aggregation of Au NPs, which can occur due to heating effects of the NPs and to the radical formation leading to the removal of the monolayer on the NP surface,^{26, 27} DLW was carried out with a range of different laser powers (0.2 mW to 4 mW) and the setup was optimized to allow for a fast and efficient activation of the photoenol moieties to minimize the aggregation. The optimum conditions were found at low laser powers (0.2-0.4 mW) (Fig. 3a). Scanning electron microscopy (SEM) images of the patterns indicate that precise immobilization of NPs was achieved in the irradiated regions (Fig. 3a). In addition, UV-Vis spectra of the prepared square patterns based on different laser powers were recorded, indicating that Au NP aggregation increases with laser power (localized particle plasmon resonances shift from 542 nm to more than 600 nm, Fig. 3b). UV-Vis spectra further indicate that at low laser power conditions Au NPs were immobilized without significant aggregation. Thus, the NP properties

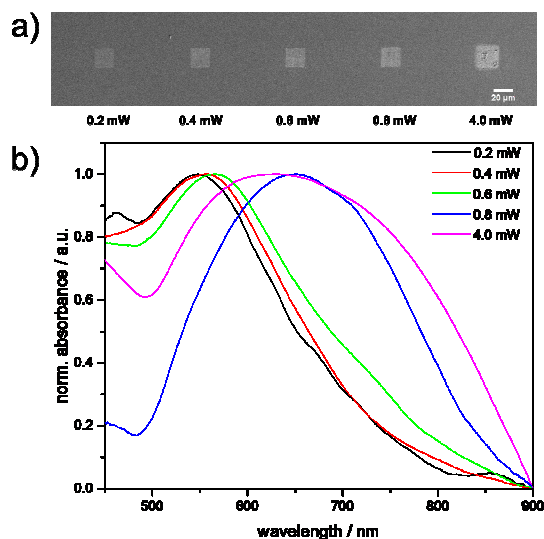


Fig. 3 (a) SEM image of square patterns, which were produced with different laser powers, from 0.2 mW to 4 mW. (b) UV-Vis spectra of the square patterns generated at the indicated laser powers showing aggregation of Au NPs at elevated laser powers (from 0.6 mW).

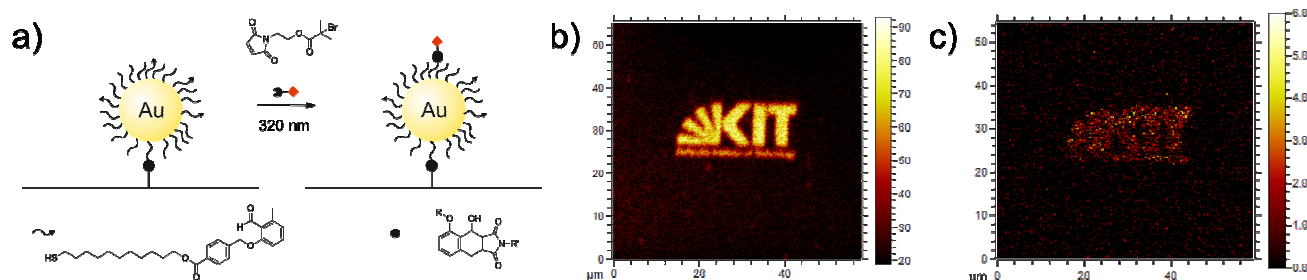


Fig. 4 (a) Light-induced Diels-Alder reaction between residual photoenol groups attached on Au NP and bromine containing maleimide. (b) ToF-SIMS image of Au^+ , Au_2S^+ , and Au_4S_2^+ . The KIT logo scanned with the DLW setup is clearly visible as it contains a high amount on thiolated Au. (c) ToF-SIMS image of the sum of ^{79}Br and ^{81}Br , indicating an increased amount of bromine onto the KIT pattern.

remained unaltered during this mild immobilization technique.

To evidence that the assembly of Au NPs is driven by covalent Diels-Alder binding, control experiments were performed utilizing non-activated components. It was shown that no patterns are obtained when either Au-MUD NPs or bare glass surfaces were used (ESI, Fig. S20-S21) and NP assembly is achieved only upon low laser power treatment (0.2-0.4 mW) of Au-MUD-PE and maleimide coated glass surfaces. At a slightly increased laser power (0.6-0.8 mW), minimal immobilization is also observed in the control experiments. Furthermore, as observed from the red shift in UV spectra (Fig. 3b), the use of increased laser power (0.6-4 mW) leads to NP agglomeration due to light absorption accompanied by Au NP induced heat generation and subsequent Au NP precipitation. This results in undesired aggregation of Au NPs, leading to a decreased pattern quality due to alteration of the immobilized Au NPs and is also an explanation for the immobilization observed in the control experiments. In contrast to other Au NP immobilization techniques on this scale such as *in situ* formation by photoreduction of gold,²⁶ the here presented technique enables the precise tailoring and thorough characterization of the NP before immobilization. As the mild fixation step does not alter the NP properties, this approach allows for a precise immobilization of tailored Au NPs.

A significant advantage of DLW driven spatially resolved surface encoding in contrast to the stamp based μCP is its ability to generate complex patterns not limited by the properties or the stamp. The DLW setup can be employed to produce virtually any desired pattern of Au NPs as shown in Fig. 4 (and in Fig. S23), where the Karlsruhe Institute of Technology (KIT) logo was written in two different sizes (approx. $30\ \mu\text{m} \times 15\ \mu\text{m}$ in Fig. 4 and approx. $60\ \mu\text{m} \times 30\ \mu\text{m}$ in Fig. S23). The presence of Au NPs within the patterns was confirmed both by SEM (ESI, Fig. S23) and time-of-flight secondary ion mass spectrometry (ToF-SIMS) (Fig. 4b). Following the immobilization of thiolated Au NPs, a set of prominent Au_xS_y peaks dominates the high mass range of the negative polarity secondary ion mass spectrum (Fig. S24). Since many of these peaks are not accompanied by other peaks at the same nominal mass, SIMS imaging with high lateral resolution is straightforward (Fig. 4b). The Au_xS_y intensity profile across the KIT logo obtained from the analysis shown in Fig. 4b demonstrates defined boundaries between immobilized and non-immobilized areas of $0.8\ \mu\text{m}$ based on the (84/16) definition (Fig. S25). Under the assumption that neighbouring areas of these boundaries are not affected by exposure, the minimum distance of two patterns and thus the resolution of this technique under these precise parameters can be estimated to be $1.6\ \mu\text{m}$. Limiting

factors of the resolution are the diffraction limit and the diffusion of activated Au NPs during the patterning process. Finally, only the photoenol moieties located in the contact area between the Au NP and the glass surface are expected to contribute to covalent NP immobilization. Assuming that the photoenol moieties are distributed evenly on the Au NPs, we expect one single covalent bond between the Au NP and the glass surface (for details of the calculation refer to the ESI) and a subset of residual photoreactive moieties remains available for further modifications. To confirm this hypothesis, the patterned surface was immersed in a solution of maleimide containing compounds under UV irradiation ($\lambda_{\text{max}} = 320\ \text{nm}$) to allow for the light-induced Diels-Alder reaction. To demonstrate the spatially resolved surface modification, a bromine containing maleimide was chosen as it allows an easy and distinct determination *via* ToF-SIMS (Fig. 4a). After irradiation, the amount of bromine (^{79}Br and ^{81}Br) within the KIT logo pattern detected by ToF-SIMS and showed an increased signal in comparison with the non-modified background (Fig. 4c). Since other peaks overlap with the bromine peaks at the same nominal masses (Fig. S24) SIMS imaging of bromine with high lateral resolution requires liquid metal ion gun burst mode as described in SI. This, in combination with the low amounts of bromine, limits the obtained image quality in Fig. 4c. However, as virtually any maleimide containing molecule can be used for postmodification of Au NP patterns an additional layer can be deposited onto the Au NPs *via* this approach.

In conclusion, the successful fabrication of 2D micropatterns using Au NPs was demonstrated by combining DLW with multiphoton induced Diels-Alder-chemistry. Au NPs were, for the first time, functionalized with photoenol precursor molecules and subsequently used for covalent, light induced surface encoding onto maleimide-coated glass substrates without aggregation of the Au NPs during the process. Residual, unreacted photoenol groups were used for further modification allowing the bottom up modification of the patterned surfaces. The combination of DLW and light-induced Diels-Alder chemistry allows for the design of virtually any desired pattern at the micron and submicron scale, which can be further modified, thus opening new avenues to design Au NP covered surfaces.

The authors acknowledge Patrice Brenner for the scanning electron microscopy measurements. The work was supported by DFG-CFN grant A5.7 and funding from the state of Baden-Württemberg (C.B.-K.) as well as the Helmholtz association in the context of the STN program (C.B.-K.). ToF-SIMS was performed within the Laboratory for Microscopy and Spectroscopy of the

Karlsruhe Nano Micro Facility (KNMF).

Notes and references

^a Center for Functional Nanostructures (CFN), Karlsruhe Institute of Technology (KIT), Wolfgang-Gaede-Str.1, 76131 Karlsruhe (Germany)

⁵ E-mail: ljiljana.fruk@kit.edu

^b Preparative Macromolecular Chemistry, Institut für Technische Chemie und Polymerchemie, Karlsruhe Institute of Technology (KIT), Engesserstrasse 18, 76128 Karlsruhe; (Germany) E-mail: christopher.barner-kowollik@kit.edu

¹⁰ ^c Institut für Biologische Grenzflächen, Karlsruhe Institute of Technology (KIT), Hermann-von-Helmholtz-Platz 1, 76344 Eggenstein-Leopoldshafen (Germany)

^d IOM-CNR Laboratorio TASC, AREA Science Park, Basovizza, 34139 Trieste (Italy)

¹⁵ ^e AREA Science Park, Padriciano 99, 34149 Trieste (Italy)

^f Institut für Nanotechnologie, Karlsruhe Institute of Technology (KIT), Hermann-von-Helmholtz-Platz 1, 76344 Eggenstein-Leopoldshafen (Germany)

²⁰ Institut für Angewandte Physik and Center for Functional Nanostructures (CFN), Karlsruhe Institute of Technology (KIT), Wolfgang-Gaede-Str. 1, 76131 Karlsruhe (Germany)

† Electronic Supplementary Information (ESI) available: Materials and methods, experimental and synthetic procedures, ESI-MS spectra and TEM images. See DOI: 10.1039/b000000x/

25

1 D. A. Giljohann, D. S. Seferos, W. L. Daniel, M. D. Massich, P. C. Patel and C. A. Mirkin, *Angew. Chem. Int. Ed.*, 2010, **49**, 3280.

2 G. A. Sotiriou, *WIREs Nanomed. Nanobiotechnol.*, 2013, **5**, 19.

3 K. E. Sapsford, W. R. Algar, L. Berti, K. B. Gemmill, B. J. Casey, E. Oh, M. H. Stewart and I. L. Medintz, *Chem. Rev.*, 2013, **113**, 1904.

4 A. A. Busnaina, J. Mead, J. Isaacs and S. Somu, *J. Nanopart. Res.*, 2013, **15**, 331.

5 B. Yu and M. Meyyappan, *Solid State Electron.*, 2006, **50**, 536.

6 A. N. Shipway, E. Katz and I. Willner, *ChemPhysChem*, 2000, **1**, 18.

7 C. Subramani, X. Yu, S. S. Agasti, B. Duncan, S. Eymur, M. Tonga and V. M. Rotello, *J. Mater. Chem.*, 2011, **21**, 14156.

8 P. M. Mendes, S. Jacke, K. Critchley, J. Plaza, Y. Chen, K. Nikitin, R. E. Palmer, J. A. Preece, S. D. Evans and D. Fitzmaurice, *Langmuir*, 2004, **20**, 3766.

9 R. J. Barsotti and F. Stellacci, *J. Mater. Chem.*, 2006, **16**, 962.

10 D. I. Rozkiewicz, D. Janczewski, W. Verboom, B. J. Ravoo and D. N. Reinhoudt, *Angew. Chem. Int. Ed.*, 2006, **45**, 5292.

11 D. I. Rozkiewicz, Y. Kraan, M. W. Werten, F. A. de Wolf, V. Subramaniam, B. J. Ravoo and D. N. Reinhoudt, *Chem. Eur. J.*, 2006, **12**, 6290.

12 D. I. Rozkiewicz, J. Gierlich, G. A. Burley, K. Gutsmedl, T. Carell, B. J. Ravoo and D. N. Reinhoudt, *ChemBioChem*, 2007, **8**, 1997.

13 I. Rianasari, M. P. de Jong, J. Huskens and W. G. van der Wiel, *Int. J. Mol. Sci.*, 2013, **14**, 3705.

14 A. Perl, D. N. Reinhoudt and J. Huskens, *Adv. Mater.*, 2009, **21**, 2257.

15 M. Deubel, G. von Freymann, M. Wegener, S. Pereira, K. Busch and C. M. Soukoulis, *Nat. Mater.*, 2004, **3**, 444.

16 M. Kaupp, A. S. Quick, C. Rodriguez-Emmenegger, A. Welle, V. Trouillet, O. Pop-Georgievski, M. Wegener and C. Barner-Kowollik, *Adv. Funct. Mater.*, 2014, **24**, 5649.

17 A. S. Quick, H. Rothfuss, A. Welle, B. Richter, J. Fischer, M. Wegener and C. Barner-Kowollik, *Adv. Funct. Mater.*, 2014, **24**, 3571.

18 H. C. Kolb, M. G. Finn and K. B. Sharpless, *Angew. Chem. Int. Ed.*, 2001, **40**, 2004.

19 T. Pauloehrli, G. Delaittre, V. Winkler, A. Welle, M. Bruns, H. G. Börner, A. M. Greiner, M. Bastmeyer and C. Barner-Kowollik, *Angew. Chem. Int. Ed.*, 2012, **51**, 1071.

20 M. Kaupp, T. Tischer, A. F. Hirschbiel, A. P. Vogt, U. Geckle, V. Trouillet, T. Hofe, M. H. Stenzel and C. Barner-Kowollik, *Macromolecules*, 2013, **46**, 6858.

21 L. Stolzer, I. Ahmed, C. Rodriguez-Emmenegger, V. Trouillet, P. Bockstaller, C. Barner-Kowollik and L. Fruk, *Chem. Commun.*, 2014, **50**, 4430.

22 T. Gruending, K. K. Oehlenschlaeger, E. Frick, M. Glassner, C. Schmid and C. Barner-Kowollik, *Macromol. Rapid Commun.*, 2011, **32**, 807.

23 J. Raula, J. Shan, M. Nuopponen, A. Niskanen, H. Jiang, E. I. Kauppinen and H. Tenhu, *Langmuir*, 2003, **19**, 3499.

24 B. Yameen, C. Rodriguez-Emmenegger, C. M. Preuss, O. Pop-Georgievski, E. Verveniots, V. Trouillet, B. Rezek and C. Barner-Kowollik, *Chem. Commun.*, 2013, **49**, 8623.

25 S. Pocovi-Martinez, M. Parreno-Romero, S. Agouram and J. Perez-Prieto, *Langmuir*, 2011, **27**, 5234.

26 I. Izquierdo-Lorenzo, S. Jradi and P. M. Adam, *RSC Adv.*, 2014, **4**, 4128.

27 A. J. Kell, A. Alizadeh, L. Yang and M. S. Workentin, *Langmuir*, 2005, **21**, 9741.

85